magnetochemistry

MDPI

Supplementary Materials

Synthesis, Structural Features and Physical Properties of a Family of Triply Bridged Dinuclear 3d-4f Complexes

Itziar Oyarzabal [1,*], Estitxu Echenique-Errandonea [1], Eider San Sebastián [1], Antonio Rodríguez-Diéguez [2], José Manuel Seco [1,*] and Enrique Colacio [2,*]

[1] Departamento de Química Aplicada, Facultad de Química, Universidad del País Vasco UPV/EHU, Paseo Manuel de Lardizabal 3, 20018 Donostia-San Sebastián, Spain; estitxu.echenique@ehu.eus (E.E.-E.); eider.sansebastian@ehu.eus (E.S.S.)

[2] Departamento de Química Inorgánica, Facultad de Ciencias, Universidad de Granada, Avda. Fuentenueva S/N, 18002 Granada, Spain; antonio5@ugr.es

* Correspondence: itziar.oyarzabal@ehu.eus (I.O.); josemanuel.seco@ehu.eus (J.M.S.); ecolacio@ugr.es (E.C.)

Table S1. Elemental analysis for complexes **1**-**15**.

Complex	Yield (%)	Formula	% C calc./found	% H calc./found	% N calc./found
1	39	$C_{24}H_{28}N_5O_{13}Br_2CuGd$	29.56/29.62	2.89/2.93	7.18/7.26
2	37	$C_{24}H_{28}N_5O_{13}Br_2CuTb$	29.51/29.44	2.89/2.91	7.17/7.23
3	41	$C_{24}H_{28}N_5O_{13}Br_2CuDy$	29.40/29.46	2.88/2.91	7.14/7.22
4	35	$C_{24}H_{28}N_5O_{13}Br_2CuEr$	29.26/29.20	2.86/2.89	7.11/7.20
5	48	$C_{26}H_{29}N_6O_{12}Br_2NiNd$	31.86/31.81	2.98/3.01	8.57/8.46
6	45	$C_{26}H_{29}N_6O_{12}Br_2NiGd$	31.44/31.50	2.94/2.95	8.46/8.53
7	52	$C_{26}H_{29}N_6O_{12}Br_2NiTb$	31.39/31.46	2.94/2.96	8.45/8.53
8	57	$C_{26}H_{29}N_6O_{12}Br_2NiDy$	31.27/31.34	2.93/2.96	8.42/8.50
9	51	$C_{26}H_{29}N_6O_{12}Br_2NiEr$	31.13/31.19	2.91/2.93	8.38/8.30
10	47	$C_{26}H_{29}N_6O_{12}Br_2NiY$	33.76/33.84	3.16/3.18	9.09/9.16
11	42	$C_{26}H_{29}N_6O_{12}Br_2CoGd$	31.43/31.51	2.94/2.95	8.46/8.47
12	50	$C_{26}H_{29}N_6O_{12}Br_2CoTb$	31.38/31.42	2.94/2.96	8.44/8.50
13	54	$C_{26}H_{29}N_6O_{12}Br_2CoDy$	31.27/31.30	2.93/2.93	8.41/8.45
14	39	$C_{26}H_{29}N_6O_{12}Br_2CoEr$	31.12/31.17	2.91/2.93	8.37/8.41
15	49	$C_{26}H_{29}N_6O_{12}Br_2CoY$	33.75/33.82	3.16/3.20	9.08/9.11

Table S2. Crystallographic data for complexes **1**-**4**.

Complex	**1**	**2**	**3**	**4**
Formula	$C_{24}H_{28}N_5O_{13}Br_2CuGd$	$C_{24}H_{28}N_5O_{13}Br_2CuTb$	$C_{24}H_{28}N_5O_{13}Br_2CuDy$	$C_{24}H_{28}N_5O_{13}Br_2CuEr$
M_r	975.11	976.78	980.36	985.12
Crystal system	Monoclinic	Monoclinic	Monoclinic	Monoclinic
Space group (no.)	P21/c (14)	*P21/c* (14)	*P21/c* (14)	*P21/c* (14)
a (Å)	13.5609(2)	13.54770(10)	13.56040(10)	13.55320(10)
b (Å)	14.9879(2)	14.93020(10)	14.90410(10)	14.87700(10)
c (Å)	20.5278(4)	20.5854(2)	20.6481(2)	20.6285(2)
α (°)	90.00	90.00	90.00	90.00
β (°)	130.7740(10)	130.9250(10)	131.0410(10)	131.0700(10)
γ (°)	90.00	90.00	90.00	90.00
V (Å^3)	3159.62(9)	3146.03(4)	3147.51(4)	3135.76(4)
Z	4	4	4	4
D_c (g cm^{-3})	2.046	2.058	2.065	2.082
μ(CuKα) (mm^{-1})[a]	5.354	15.354	16.999	9.282
T (K)	100(2)	100(2)	100(2)	100(2)
Observed reflections	6368(5853)	6320 (6124)	6323(5908)	6294(5881)
R_{int}	0.0181	0.0287	0.0401	0.0302
Parameters	429	429	428	428
GOF	1.047	1.055	1.041	1.048
R_1[b,c]	0.0201(0.0170)	0.0215 (0.0206)	0.0327(0.0297)	0.0252(0.0229)
wR_2[d]	0.0385(0.0375)	0.0494 (0.0490)	0.0779(0.0752)	0.0567(0.0554)
Largest difference in peak and hole (e Å^{-3})	0.487 and -0.364	0.410 and -0.597	1.436 and -0.886	0.909 and -0.743

[a] μ(MoKα) (mm^{-1}) in **1**. [b] $R_1 = \Sigma||F_o| - |F_c||/\Sigma|F_o|$. [c] Values in parentheses for reflections with $I > 2\sigma(I)$. [d] $wR_2 = \{\Sigma[w(F_o^2 - F_c^2)^2] / \Sigma[w(F_o^2)^2]\}^{1/2}$.

Table S3. Crystallographic data for complexes **5**-**10**.

Complex	**5**	**6**	**7**	**8**	**9**	**10**
Formula	$C_{26}H_{29}N_6O_{12}Br_2NiNd$	$C_{26}H_{29}N_6O_{12}Br_2NiGd$	$C_{26}H_{29}N_6O_{12}Br_2NiTb$	$C_{26}H_{29}N_6O_{12}Br_2NiDy$	$C_{26}H_{29}N_6O_{12}Br_2NiEr$	$C_{26}H_{29}N_6O_{12}Br_2NiY$
M_r	980.32	993.33	995.00	998.58	1003.34	924.99
Crystal system	triclinic	triclinic	triclinic	triclinic	triclinic	triclinic
Space group (no.)	P-1 (2)	P-1 (2)	P-1 (2)	P-1 (2)	P-1 (2)	P-1 (2)
a (Å)	10.217(3)	10.1426(4)	10.2484(13)	10.1327(3)	10.1226(5)	10.1465(5)
b (Å)	13.043(5)	12.9916(5)	13.084(2)	12.9880(6)	12.9640(6)	12.9861(5)
c (Å)	14.137(5)	14.0258(6)	14.137(2)	13.9878(3)	13.9826(4)	13.9911(8)
a (°)	76.953(10)	77.173(4)	76.894(4)	77.099(3)	76.958(4)	76.955(4)
β (°)	70.394(10)	69.930(4)	70.371(4)	69.968(2)	69.879(4)	69.933(5)
γ (°)	68.948(10)	68.995(4)	68.686(4)	68.965(4)	68.983(5)	68.811(4)
V (Å^3)	1644.4(10)	1610.20(11)	1651.4(4)	1603.63(10)	1597.33(13)	1603.61(14)
Z	2	2	2	2	2	2
D_c (g cm^{-3})	1.980	2.049	2.001	2.068	2.086	1.916
μ(MoKα) (mm^{-1})[a]	4.633	5.179	5.183	5.462	9.028	4.951
T (K)	100(2)	100(2)	100(2)	100(2)	100(2)	100(2)
Observed reflections	5709(4411)	5666(5220)	5682(4437)	5650(5280)	6231(5469)	5651(5031)
R_{int}	0.1119	0.0267	0.0715	0.0152	0.0380	0.0220
Parameters	438	438	438	438	438	438
GOF	1.028	1.062	1.046	1.042	1.065	1.027
R_1[b,c]	0.0848(0.0644)	0.0345(0.0308)	0.0635(0.0422)	0.0205(0.0182)	0.0499(0.0428)	0.0319(0.0264)
wR_2[d]	0.1721(0.1579)	0.0770(0.0742)	0.0962(0.0882)	0.0408(0.0400)	0.1236(0.1186)	0.0586(0.0564)
Largest difference in peak and hole (e Å^{-3})	2.709 and -1.549	1.791 and -1.565	1.574 and -0.839	0.732 and -0.621	2.071 and -1.249	0.562 and -0.369

[a] μ(CuKα) (mm^{-1}) in **9**. [b] $R_1 = \Sigma||F_o| - |F_c||/\Sigma|F_o|$. [c] Values in parentheses for reflections with $I > 2\sigma(I)$. [d] $wR_2 = \{\Sigma[w(F_o^2 - F_c^2)^2] / \Sigma[w(F_o^2)^2]\}^{1/2}$.

Table S4. Crystallographic data for complexes **11**-**15**.

Complex	**11**	**12**	**13**	**14**	**15**
Formula	$C_{26}H_{29}N_6O_{12}Br_2CoGd$	$C_{26}H_{29}N_6O_{12}Br_2CoTb$	$C_{26}H_{29}N_6O_{12}Br_2CoDy$	$C_{26}H_{29}N_6O_{12}Br_2CoEr$	$C_{26}H_{29}N_6O_{12}Br_2CoY$
Mr	993.55	995.22	998.80	1003.56	925.21
Crystal system	triclinic	triclinic	triclinic	triclinic	triclinic
Space group (no.)	P-1 (2)	P-1 (2)	P-1 (2)	P-1 (2)	P-1 (2)
a (Å)	10.191(5)	10.1820(4)	10.1815(6)	10.1576(4)	10.189(3)
b (Å)	13.024(5)	13.0186(6)	12.9982(6)	12.9970(6)	12.996(3)
c (Å)	14.101(5)	14.0454(6)	14.0503(7)	14.0319(7)	14.056(4)
a (°)	76.932(5)	76.909(4)	76.876(4)	76.836(4)	76.808(3)
β (°)	69.771(5)	69.758(3)	69.709(5)	69.859(4)	69.730(3)
γ (°)	69.146(5)	69.177(4)	69.050(5)	69.147(4)	69.011(3)
V (Å^3)	1629.7(12)	1621.29(11)	1617.42(14)	1613.55(13)	1618.5(7)
Z	2	2	2	2	2
D_c (g cm^{-3})	2.025	2.039	2.051	2.066	1.898
μ(MoKα) (mm^{-1})[a]	5.048	5.210	5.346	12.239	4.836
T (K)	100(2)	100(2)	100(2)	100(2)	100(2)
Observed reflections	8444(7775)	6633(6162)	6537(5819)	6043(5720)	7300(5837)
Rint	0.0254	0.0172	0.0277	0.0367	0.0408
Parameters	438	438	438	438	438
GOF	1.168	1.042	1.034	1.056	1.045
R_1[b,c]	0.0240 (0.0208)	0.0246(0.0216)	0.0329(0.0272)	0.0332(0.0313)	0.0510 (0.0366)
wR_2[d]	0.0497 (0.0480)	0.0461(0.0449)	0.0521(0.0493)	0.0826(0.0812)	0.0745(0.0692)
Largest difference in peak and hole (e Å^{-3})	0.790 and -0.956	0.563 and -0.652	0.900 and -0.877	0.917 and -1.026	0.720 and -0.454

[a] μ(CuKα) (mm^{-1}) in **14**. [b] $R_1 = \Sigma||F_o| - |F_c||/\Sigma|F_o|$. [c] Values in parentheses for reflections with $I > 2\sigma(I)$. [d] $wR_2 = \{\Sigma[w(F_o^2 - F_c^2)^2] / \Sigma[w(F_o^2)^2]\}^{1/2}$.

Table S5. Selected bond distances (Å) and angles (°) for complexes **1**-**4**.

Complex	1	2	3	4
Ln(1)-Cu(1)	3.383(1)	3.370(1)	3.364(1)	3.353(1)
Ln(1)-O(1A)	2.374(2)	2.357(2)	2.350(2)	2.326(2)
Ln(1)-O(2A)	2.367(2)	2.354(2)	2.349(2)	2.326(2)
Ln(1)-O(3A)	2.404(2)	2.390(2)	2.378(2)	2.358(2)
Ln(1)-O(4A)	2.389(2)	2.371(2)	2.360(2)	2.337(2)
Ln(1)-O(2P)bridge	2.290(2)	2.280(2)	2.260(2)	2.254(2)
Ln(1)-O(1C)nitrate	2.479(2)	2.506(2)	2.493(2)	2.472(2)
Ln(1)-O(2C)nitrate	2.523(2)	2.459(2)	2.450(3)	2.426(2)
Ln(1)-O(1D)nitrate	2.486(2)	2.469(2)	2.454(2)	2.429(2)
Ln(1)-O(2D)nitrate	2.534(2)	2.533(2)	2.517(3)	2.494(2)
Cu(1)-N(1A)	2.024(2)	2.023(2)	2.022(3)	2.019(2)
Cu(1)-N(2A)	2.017(2)	2.018(2)	2.024(3)	2.019(2)
Cu(1)-O(2A)	2.057(2)	2.052(2)	2.049(2)	2.044(2)
Cu(1)-O(3A)	2.010(2)	2.007(2)	2.006(2)	1.999(2)
Cu(1)-O(1P)bridge	2.126(2)	2.134(2)	2.140(3)	2.146(2)
Ln(1)-O(2A)-Cu(1)	99.51(6)	99.56(6)	99.57(9)	100.01(7)
Ln(1)-O(3A)-Cu(1)	99.68(6)	99.70(6)	99.92(9)	100.29(7)
O(2A)-Ln(1)-O(3A)	69.80(5)	70.02(5)	70.13(8)	70.03(6)
O(2A)-Ln(1)-O(2P)bridge	80.33(5)	80.58(6)	80.62(9)	80.92(6)
O(3A)-Ln(1)-O(2P)bridge	80.74(5)	80.99(6)	81.01(9)	81.32(6)
O(2A)-Cu(1)-O(3A)	84.32(6)	84.19(6)	84.10(9)	83.32(7)
O(2A)-Cu(1)-O(1P)bridge	96.50(6)	96.11(6)	95.76(10)	95.72(7)
O(3A)-Cu(1)-O(1P)bridge	93.42(6)	93.15(7)	92.73(10)	92.78(7)

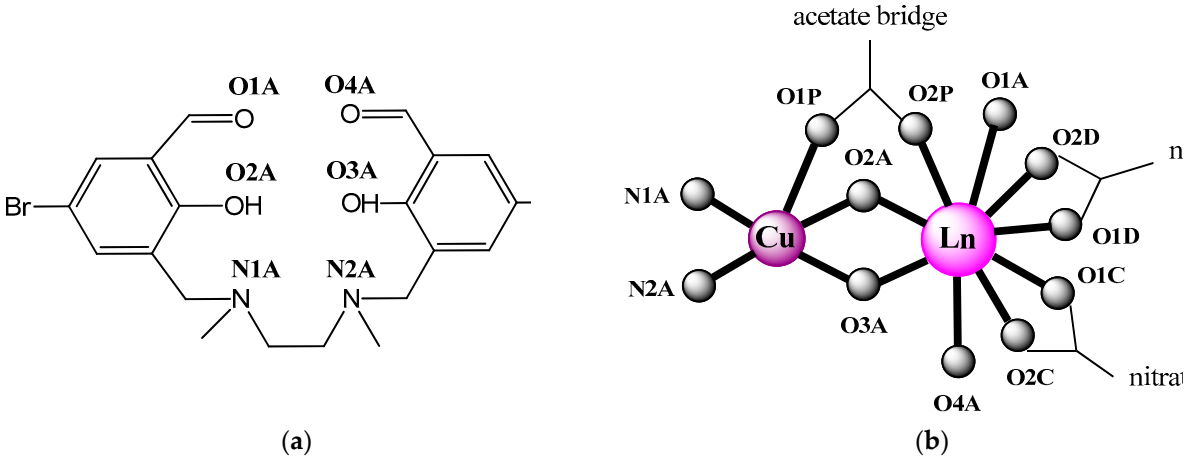

Scheme S1. Ligand scheme (**a**) and labelling scheme (**b**) used in Table S5 for complexes 1-4.

Table S6. Selected bond distances (Å) and angles (°) for complexes **5**-**15**.

Complex	5	6	7	8	9	10	11	12	13	14	15
Ln(1)-M(1)	3.437(2)	3.418(1)	3.414(1)	3.399(1)	3.385(1)	3.393(1)	3.431(2)	3.420(1)	3.414(1)	3.395(1)	3.408(1)
Ln(1)-O(1A)	2.428(6)	2.393(3)	2.381(4)	2.365(2)	2.341(4)	2.352(2)	2.403(2)	2.404(2)	2.373(2)	2.353(2)	2.359(2)
Ln(1)-O(2A)	2.387(5)	2.341(3)	2.341(4)	2.321(2)	2.299(4)	2.304(2)	2.357(2)	2.352(2)	2.373(2)	2.306(2)	2.321(2)
Ln(1)-O(3A)	2.428(6)	2.379(3)	2.356(4)	2.352(2)	2.327(4)	2.339(2)	2.366(2)	2.341(2)	2.338(2)	2.316(2)	2.329(2)
Ln(1)-O(4A)	2.468(7)	2.422(3)	2.407(5)	2.400(2)	2.377(4)	2.390(2)	2.420(2)	2.390(2)	2.391(2)	2.375(2)	2.380(2)
Ln(1)-O(2P)bridge	2.369(7)	2.320(3)	2.285(4)	2.284(2)	2.282(4)	2.275(2)	2.328(2)	2.308(2)	2.287(2)	2.275(2)	2.279(2)
Ln(1)-O(1C)nitrate	2.527(6)	2.481(3)	2.470(4)	2.451(2)	2.428(4)	2.436(2)	2.495(2)	2.468(2)	2.447(2)	2.421(2)	2.451(2)
Ln(1)-O(2C)nitrate	2.524(6)	2.505(3)	2.507(5)	2.490(2)	2.471(4)	2.478(2)	2.515(2)	2.491(2)	2.481(2)	2.457(2)	2.486(2)
Ln(1)-O(1D)nitrate	2.527(6)	2.493(3)	2.471(4)	2.464(2)	2.429(4)	2.444(2)	2.481(2)	2.481(2)	2.463(2)	2.433(2)	2.437(2)
Ln(1)-O(2D)nitrate	2.537(7)	2.511(3)	2.511(4)	2.492(2)	2.473(4)	2.477(2)	2.501(2)	2.506(2)	2.494(2)	2.479(3)	2.475(2)
M(1)-N(1A)	2.087(6)	2.105(3)	2.103(4)	2.102(2)	2.108(4)	2.100(2)	2.174(2)	2.152(2)	2.166(3)	2.173(3)	2.167(3)
M(1)-N(2A)	2.094(8)	2.103(3)	2.101(5)	2.102(2)	2.101(5)	2.104(2)	2.152(2)	2.164(2)	2.155(3)	2.150(3)	2.154(3)
M(1)-O(2A)	2.056(6)	2.063(3)	2.053(4)	2.061(2)	2.054(4)	2.058(2)	2.055(2)	2.203(2)	2.055(2)	2.050(2)	2.049(2)
M(1)-O(3A)	2.134(5)	2.127(3)	2.136(4)	2.126(2)	2.124(4)	2.130(2)	2.202(2)	2.056(2)	2.198(2)	2.194(2)	2.200(2)
M(1)-O(1P)bridge	2.051(6)	2.067(3)	2.069(4)	2.060(2)	2.066(4)	2.060(2)	2.064(2)	2.058(2)	2.064(2)	2.061(2)	2.061(2)
M(1)-N(1F)	2.084(8)	2.070(4)	2.084(6)	2.068(2)	2.060(5)	2.068(2)	2.114(2)	2.113(2)	2.114(3)	2.115(3)	2.113(3)
Ln(1)-O(2A)-M(1)	101.1(2)	101.65(10)	101.81(14)	101.57(7)	101.94(15)	101.99(7)	101.87(6)	97.27(7)	102.05(9)	102.24(9)	102.29(9)
Ln(1)-O(3A)-M(1)	97.6(2)	98.51(10)	98.81(15)	98.63(7)	98.94(14)	98.71(7)	97.29(6)	101.94(7)	97.59(8)	97.64(9)	97.55(8)
O(2A)-Ln(1)-O(3A)	70.09(18)	70.27(9)	70.39(13)	70.69(6)	70.79(13)	70.76(6)	70.85(6)	71.07(6)	70.98(7)	71.24(8)	71.11(8)
O(2A)-Ln(1)-O(2P)bridge	76.75(19)	76.91(10)	77.34(14)	77.05(6)	77.08(14)	76.88(7)	77.50(6)	84.11(6)	77.64(8)	77.70(8)	77.61(8)
O(3A)-Ln(1)-O(2P)bridge	84.5(2)	85.05(10)	84.72(16)	85.19(6)	85.75(14)	85.37(7)	84.07(6)	77.59(6)	84.29(8)	84.79(9)	84.39(8)
O(2A)-M(1)-O(3A)	82.6(2)	80.83(10)	80.48(15)	80.42(7)	79.77(15)	79.87(7)	79.94(6)	79.58(7)	79.11(8)	78.66(9)	78.95(8)
O(2A)-M(1)-O(1P)bridge	100.9(2)	101.37(11)	101.15(16)	101.46(7)	101.15(16)	101.33(8)	104.81(6)	104.91(7)	104.89(9)	104.69(10)	104.76(9)
O(3A)-M(1)-O(1P)bridge	86.0(2)	85.63(11)	85.57(15)	85.50(7)	85.44(16)	85.53(7)	85.32(6)	85.40(7)	85.38(8)	85.32(9)	85.28(9)

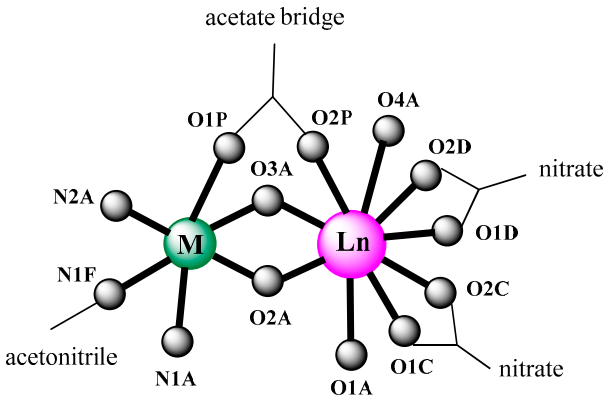

Scheme S2. Labelling scheme used in Table S6 for complexes **5**-**15** (M = Ni/Co).

Table S7. Shape measures for Cu^{II} coordination environments in compounds **1**-**4**.

Complex	Pentagon	Vacant Octahedron	Trigonal Bipyramid	Square Pyramid	Johnson Trigonal Bipyramid
1	31.231	1.648	3.476	0.694	6.363
2	31.106	1.631	3.503	0.723	6.382
3	31.115	1.659	3.517	0.755	6.423
4	30.958	1.742	3.482	0.783	6.428

Table S8. Shape measures for Ni^{II} coordination environments in compounds **5**-**10**.

Complex	Octahedron	Trigonal Prism	% Octahedron	% Deviation Path
5	0.927	10.884	77.1	2.7
6	0.962	10.929	76.7	3.2
7	1.011	10.804	76.1	3.4
8	1.004	10.798	76.2	3.3
9	1.027	10.761	75.9	3.4
10	1.034	10.750	75.8	3.4

Shape measures relative to other reference polyhedral are significantly larger.

Table S9. Shape measures for Co^{II} coordination environments in compounds **11**-**15**.

Complex	Octahedron	Trigonal Prism	% Octahedron	% Deviation Path
11	1.318	10.061	72.7	3.9
12	1.351	9.990	72.4	3.9
13	1.384	9.974	72.0	4.2
14	1.400	9.972	71.9	4.4
15	1.318	9.954	71.9	4.3

Shape measures relative to other reference polyhedral are significantly larger.

Table S10. Shape measures for the LnO_9 coordination environments in compounds **1**-**15**.

Complex	Capped sq. Antiprism (JCSAPR-9)	Capped sq. Antiprism (CSAPR-9)	Tricapped Trig. Prism (JTCTPR-9)	Tricapped Trig. Prism (TCTPR-9)	Muffin (MFF-9)
1	2.214	**1.460**	2.967	1.850	1.615
2	2.113	**1.398**	2.933	1.835	1.584
3	2.045	**1.340**	2.922	1.824	1.535
4	1.948	**1.262**	2.839	1.780	1.482
5	2.940	1.607	3.898	2.690	**1.582**
6	2.761	**1.428**	3.525	2.402	1.428
7	2.742	**1.449**	3.438	2.373	1.513
8	2.699	**1.385**	3.312	2.252	1.436
9	2.708	**1.379**	3.244	2.155	1.445
10	2.693	**1.366**	3.246	2.181	1.430
11	2.787	**1.479**	3.549	2.488	1.503
12	2.785	**1.474**	3.470	2.449	1.509
13	2.741	**1.445**	3.364	2.362	1.496
14	2.729	**1.421**	3.248	2.233	1.494
15	2.712	**1.419**	3.282	2.282	1.497

Shape measures relative to other reference polyhedral are significantly larger.

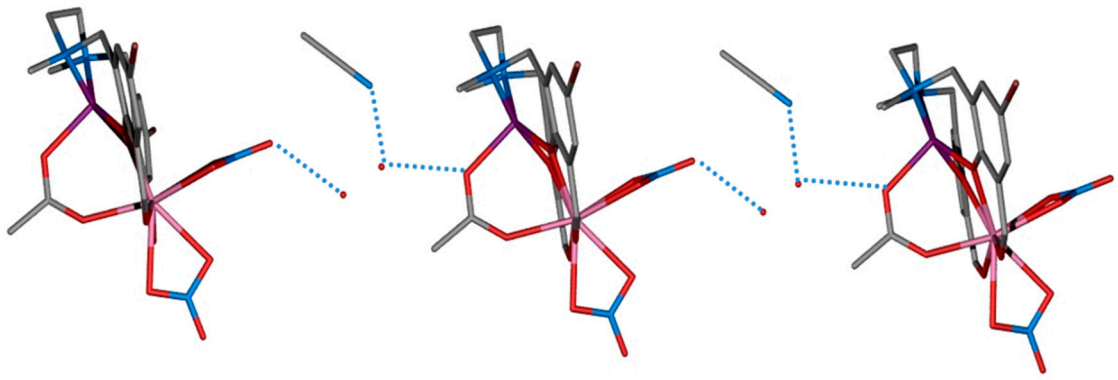

Figure S1. A perspective view of the structure of **1**-**4** together with intermolecular (blue dotted lines) hydrogen bonds.

Table S11. *Direct current* magnetic data for compounds **1**-**15**.

Complex	Ground State of Ln(III) Ion	χ_MT theor.[a] at 300K/exp. at 300 K/exp. at lowest Temperature K ($cm^3 \cdot K \cdot mol^{-1}$)	M theor.[b]/M exp. at 2 K ($N\mu_B$)
1	$^8S_{7/2}$, g = 2	8.27/8.25/9.31	7.91/8
2	$^7F_6$, g_J = 3/2	12.19/12.14/10.70	10/5.92
3	$^6H_{15/2}$, g_J = 4/3	14.54/14.87/13.99	11/6.04
4	$^4I_{15/2}$, g_J = 6/5	11.85/12.06/7.93	10/6.89
5	$^4I_{9/2}$, g_J = 8/11	2.64/2.62/1.23	5.27/2.4
6	$^8S_{7/2}$, g = 2	9.38/8.875/10.67	9.01/9
7	$^7F_6$, g_J = 3/2	12.82/13.6/10.40	11/9.2
8	$^6H_{15/2}$, g_J = 4/3	15.17/16.0/11.60	12/10.61
9	$^4I_{15/2}$, g_J = 6/5	12.48/12.70/6.09	11/6.2
10	-	1.23/1/0.957	1.57/2
11	$^8S_{7/2}$, g = 2	11.09/9.75/10.90	9.79/10
12	$^7F_6$, g_J = 3/2	13.69/15.59/10.64	12/7.87
13	$^6H_{15/2}$, g_J = 4/3	16.04/16.01/9.27	13/8.49
14	$^4I_{15/2}$, g_J = 6/5	13.35/13.66/7.05	12/8.05
15	-	2.72/1.875/1.82	2.6/3

[a] $\chi_M T = \frac{N\beta^2}{3k}\{g_j^2 J(J+1) + g_M^2 S(S+1)\}$ ($M = Cu^{II}, Ni^{II}, Co^{II}$)

[b] $J = L + S_T$; $S_T = S_{Ln} + S_M$; $g_j = \frac{3}{2} + \frac{S_T(S_T+1) - L(L+1)}{2J(J+1)}$; $M_s = g_J J N \mu_B$

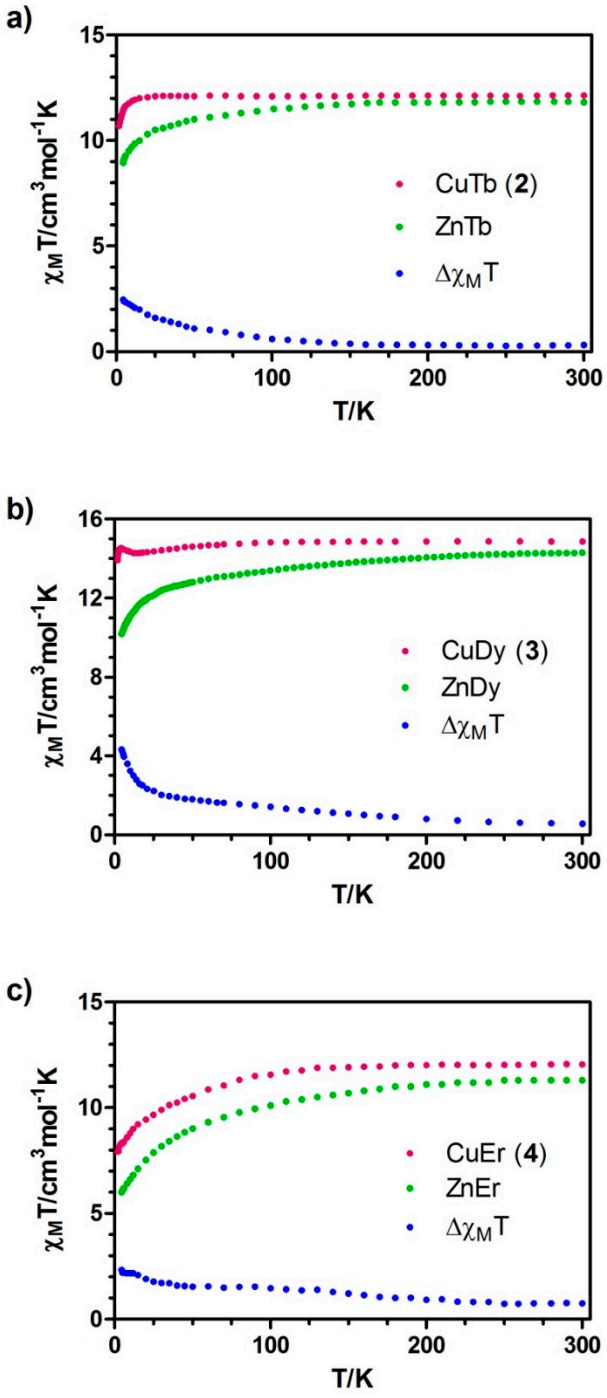

Figure S2. Temperature dependence of the $\chi_M T$ product and the difference $\Delta\chi_M T = \chi_M T_{(CuLn)} - \chi_M T_{(ZnLn)}$ for complexes **2** (**a**), **3** (**b**) and **4** (**c**).

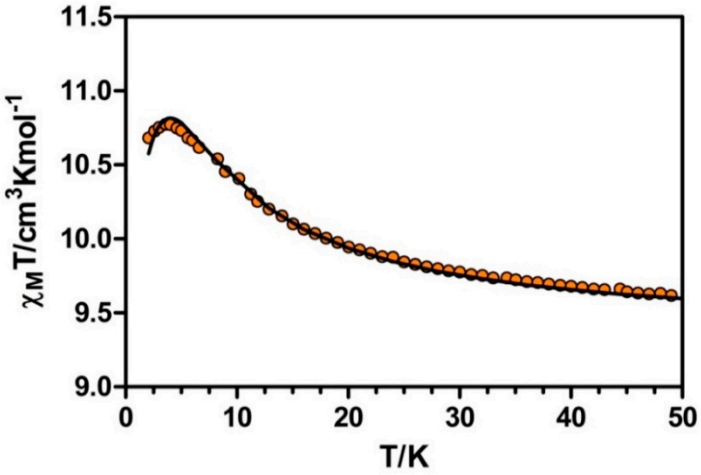

Figure S3. Temperature dependence of $\chi_M T$ product at 1000 Oe for **6** in the low temperature region. The black solid line shows the best fit.

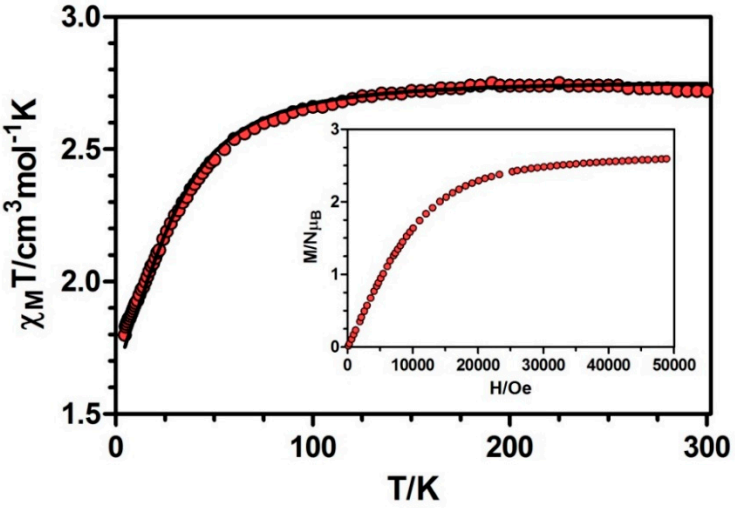

Figure S4. Temperature dependence of the $\chi_M T$ product at 1000 Oe for complex **15**. The black solid line represents the best fit. Inset: *M* versus *H* plot for **15** at 2 K.

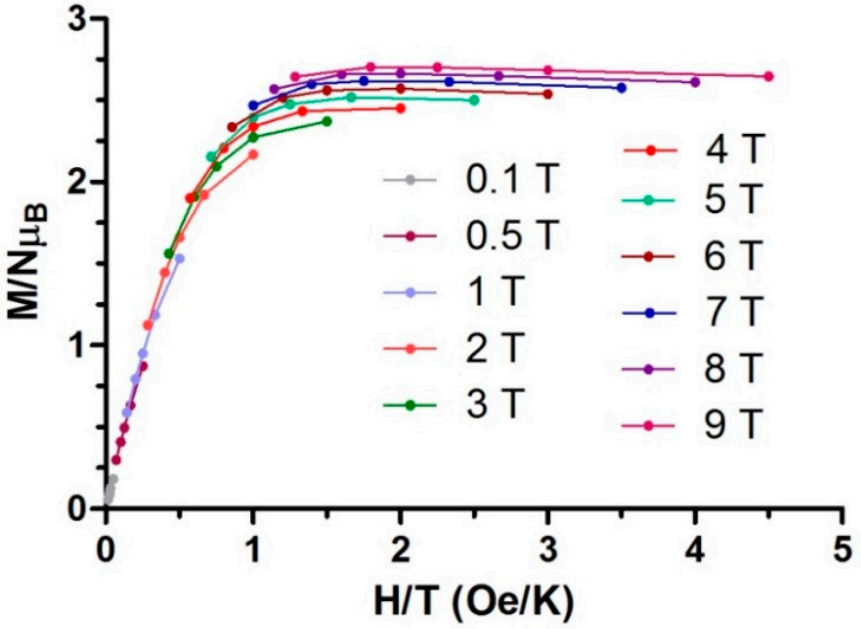

Figure S5. *M* vs. *H*/*T* plot for **15**. Solid lines are guides for the eye.

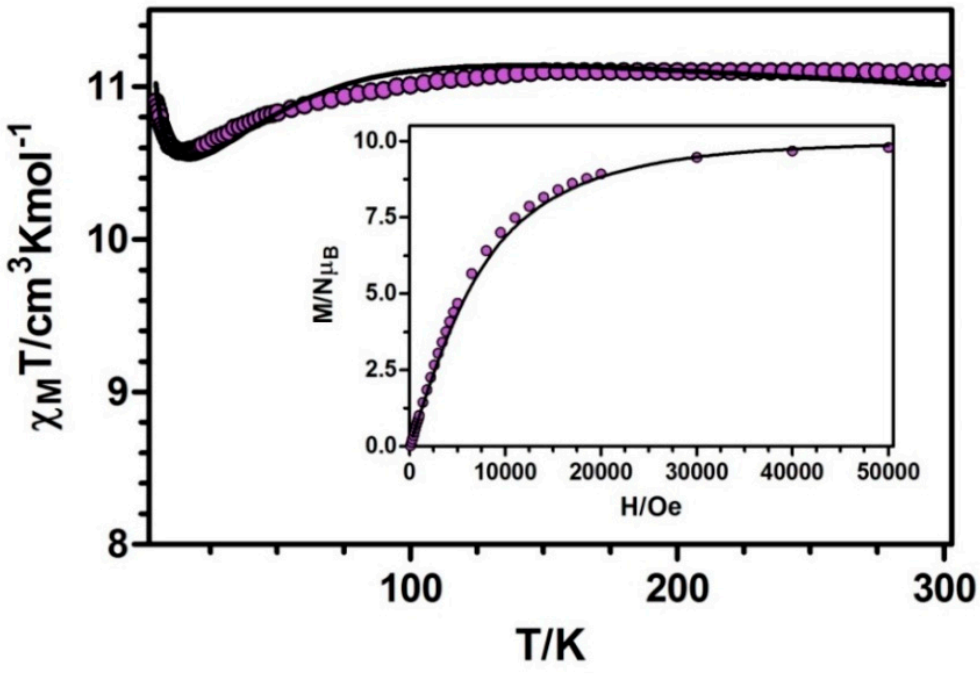

Figure S6. Temperature dependence of $\chi_M T$ product at 1000 Oe for **11**. The black solid line shows the best fit. Inset: *M* versus *H* plot for **11** at 2 K. The black solid line represents the Brillouin function for a pair of non-interacting Co^{II} ($S = 3/2$ and $g = 2.06$) and Gd^{III} ions ($S = 7/2$ and $g = 2.06$).

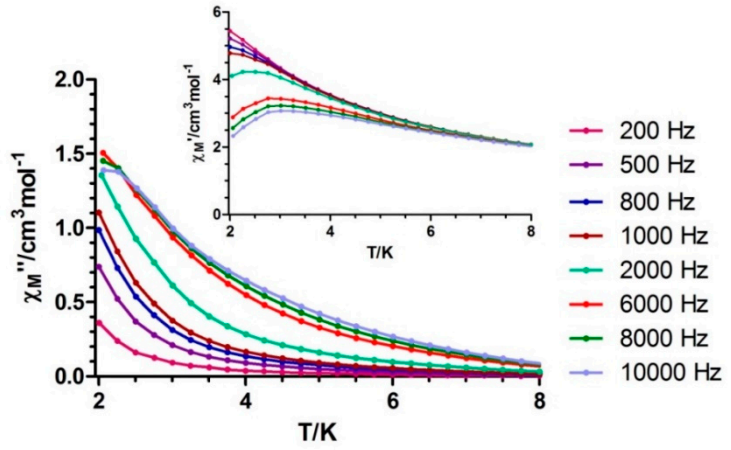

(**a**)

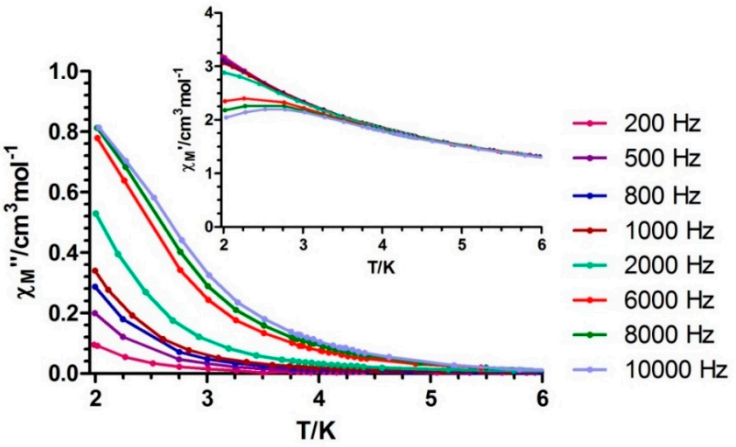

(**b**)

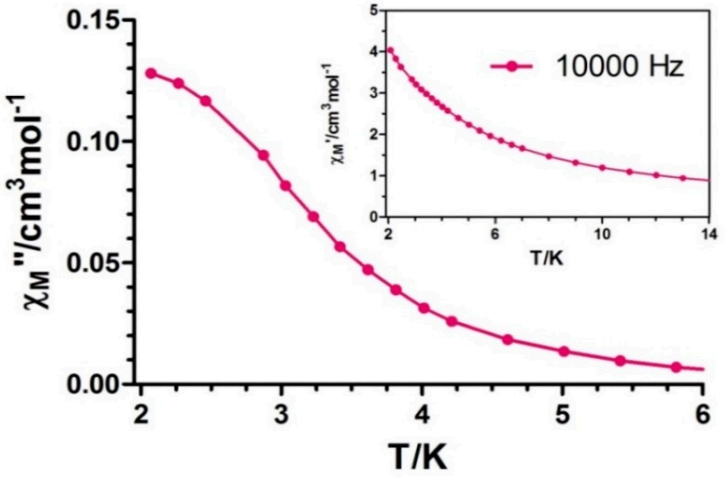

(**c**)

Figure S7. Temperature dependence of in-phase χ_M' (insets) and out-of phase χ_M'' components of the *alternating current* susceptibility for complexes **8** (**a**), **9** (**b**) and **13** (**c**) under an applied field of 1000 Oe.

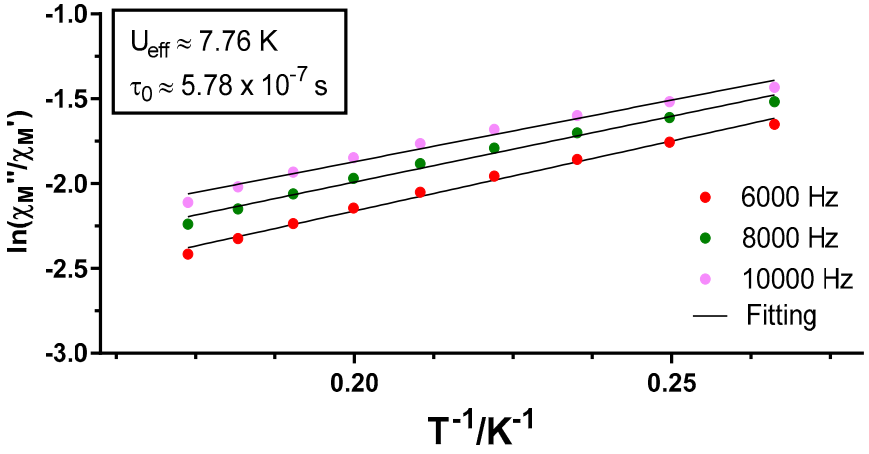

(**a**)

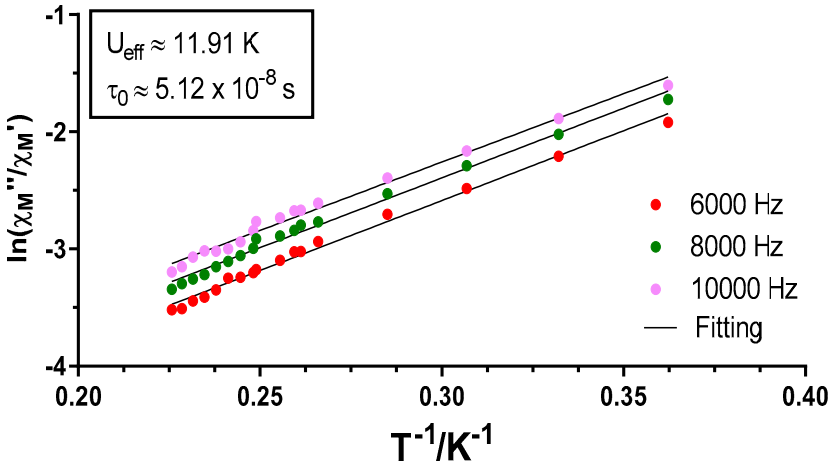

(**b**)

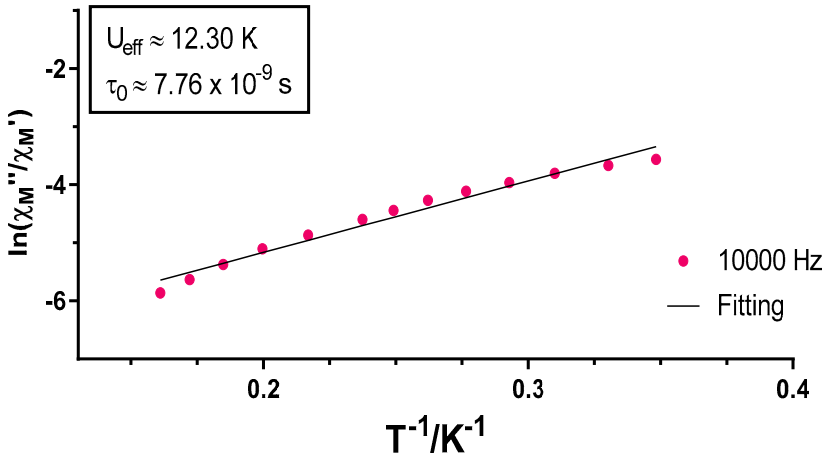

(**c**)

Figure S8. Plot of $\ln(\chi_M''/\chi_M')$ versus 1/T at different frequencies for complexes **8** (**a**), **9** (**b**) and **13** (**c**) under an applied field of 1000 Oe. The solid lines represent the linear fit with $\ln(\chi_M''/\chi_M') = \ln(2\pi\nu\tau_0) + E_a/k_BT$.

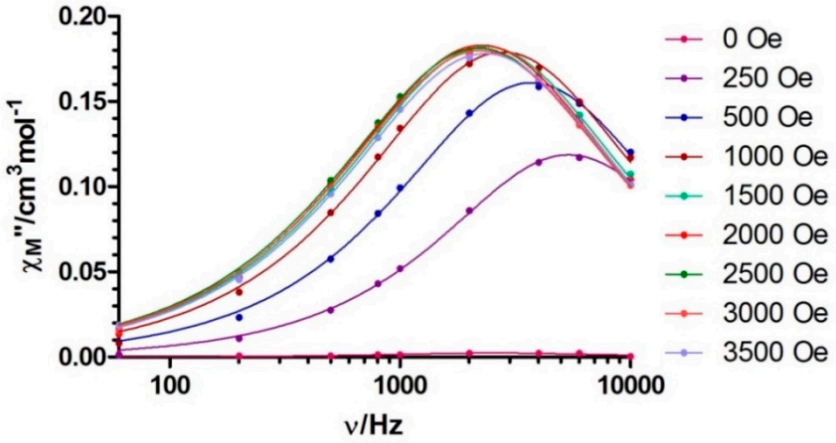

Figure S9. Field dependence of the out-of-phase signal *vs*. frequency at 4 K for **15**.

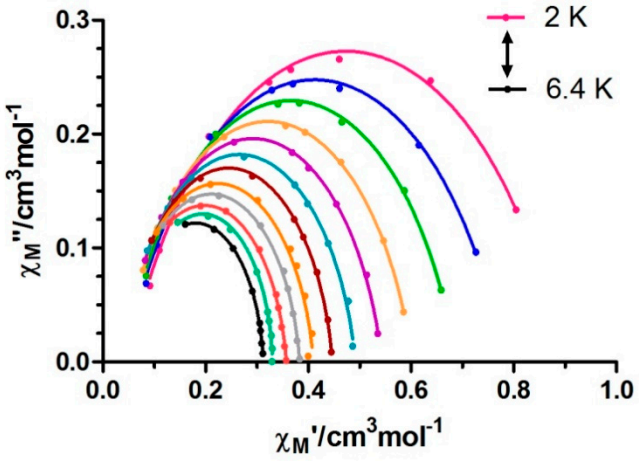

Figure S10. Cole-Cole plot for **15**.

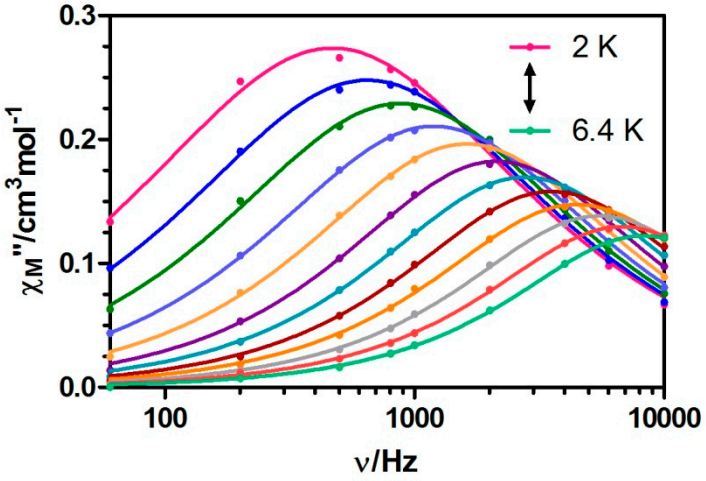

Figure S11. Variable-temperature frequency dependency of χ_M'' signal for **15**.

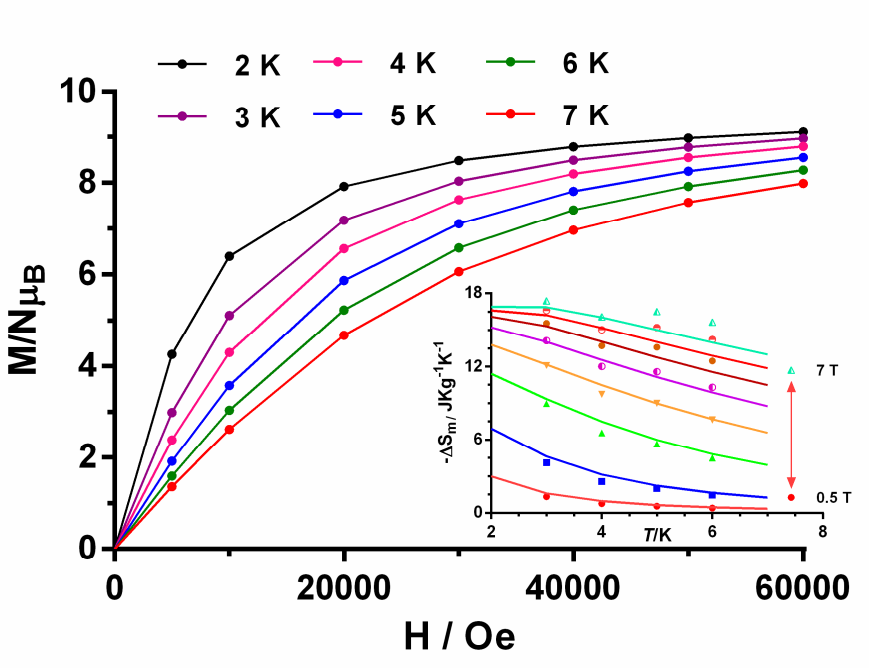

Figure S12. Field dependence of the magnetization at different temperatures for **6**. The solid lines are a guide to the eye. Inset: Magnetic entropy changes extracted from the experimental magnetization data for **6**. The solid lines represent the values calculated from the magnetic parameters (*J*, *g* and *zJ*) indicated in the text.